



# Experimental study of tool wear and its effects on cutting process of ultrasonic-assisted milling of Ti6Al4V

Qimeng Liu<sup>1</sup> · Jinkai Xu<sup>1</sup> · Huadong Yu<sup>1</sup>

Received: 2 March 2020 / Accepted: 2 June 2020 / Published online: 14 June 2020  
© Springer-Verlag London Ltd., part of Springer Nature 2020

## Abstract

Ti6Al4V is usually considered difficult to machine, and therefore, it causes severe tool wear and shortens tool life while being machined during conventional milling, leading to loss of quality and accuracy of the machined parts. In this paper, the experiment of ultrasonic-assisted milling of Ti6Al4V was conducted to study the tool wear mechanism in ultrasonic-assisted milling process and investigate the influence of the wear variable state of tool continuous cutting on the cutting process in ultrasonic-assisted milling and conventional milling. The experimental analysis showed that oxidation wear, adhesive wear, and diffusion wear occurred in ultrasonic-assisted milling; however, longer tool life was achieved when machining under the same conditions as compared to that of conventional milling. On the other hand, the curl angle of chip generated from ultrasonic-assisted milling was smaller than that from conventional milling in the same wear time. In addition, the burr produced by ultrasonic-assisted milling was not obvious, and under the coupling effect of ultrasonic-assisted milling, lower cutting force, improved surface roughness, and lower cutting temperature were obtained as compared to those of conventional milling under the same wear time.

**Keywords** Exoskeleton arm teleoperation · Magnetic drive pump · Pneumatic force-feedback · Hybrid fuzzy control

## 1 Introduction

Ti6Al4V is considered as a difficult-to-cut material because of its low thermal conductivity, low elastic modulus, and high chemical activity at high temperature, which can accelerate tool wear and reduce tool service life in the process of machining. Meanwhile, rapid tool wear results in poor accuracy, low efficiency, high cost, and poor surface quality of Ti6Al4V parts during machining [1–5]. Ultrasonic-assisted machining is a significant way to solve this kind of problem. Professor Zhao Bo conducted finite element simulation by opening a spiral groove in the conical section of the conical composite horn, analyzed the influence of ultrasonic incidence angle on the vibration mode and the influence of torsional to longitudinal ratio in the longitudinal to torsional composite vibration, and analyzed the influence of incidence angle on the machining effect through ultrasonic machining titanium alloy test. It

provides theoretical basis for the design of the longitudinal torsional composite horn [6]. Li Pengtao applied ultrasonic vibration in the axial direction of the tool and the horizontal direction of the workpiece and analyzed the milling surface morphology, cutting force, and tool wear under different ultrasonic vibration directions, to explore the influence of surface morphology on friction characteristics and the influence of ultrasonic vibration on the sawtooth degree of chips, so as to obtain the appropriate vibration mode and processing parameters [7]. According to Professor Kang Renke's experiments, diamond cutting tools play an important role in ultra-precision machining because of their excellent properties, physical and mechanical material characteristics. Cutting edges can be sharpened to nanometer level [8]. Professor Dong Guojun carried out molecular dynamic simulation and experimental research on tool wear mechanism in cutting aluminum alloy [9]. Different levels of tool wear have a direct impact on the quality of treated Ti6Al4V material. As a matter of fact, the cutting edge of the tool is subject to a sharpening process at the initial stage of wear, and every edge fails to achieve an optimal performance during machining showing a direct impact on elastic deformation zone, which is not the optimal machining stage [10–15]. Subsequently, the blade becomes sharpest at the normal wear stage, leading to an

✉ Huadong Yu  
172024452@qq.com

<sup>1</sup> Ministry of Education Key Laboratory for Cross-Scale Micro and Nano Manufacturing, Changchun University of Science and Technology, Changchun 130022, China

optimum cutting performance. As a result, the best surface quality and optimum accuracy can be obtained at this stage. Then severe tool wear begins to occur, and the blade gradually becomes blunt and even collapsed, which exhibits the worst performance no matter in accuracy or quality [16–24].

Therefore, in this paper, an experiment of ultrasonic-assisted milling of Ti6Al4V is carried out to investigate the mechanism of tool wear and explore the influence of the variable state of tool wear on the cutting process in ultrasonic-assisted milling and conventional milling. Furthermore, the law of influence of tool wear life and the effect of different levels of tool wear during ultrasonic-assisted milling on chip shape are investigated, providing the basis for machining of Ti6Al4V parts in practice.

## 2 Analysis of ultrasonic-assisted milling mechanism

### 2.1 Formation mechanism of sawtooth chip

As shown in Fig. 1, the second deformation area was formed due to the extrusion and friction between the front cutter face and the workpiece. In this area, the bottom layer of the chip gradually slid near the rake face, and hence, separation of material gradually slowed down at a certain time. On the other hand, the temperature of the tool-chip interface rose sharply because of friction, which directly affected the service life of the tool. In this process, change in physical and dynamic conditions could cause plastic deformation to occur. Friction at the workpiece-tool-chip interface was a key factor for milling of Ti6Al4V, resulting in high temperature, high stress, and chemical reaction, and hence, tool wear occurred [6].

When the thermal softening effect of the material in the shear zone is greater than that of strain hardening and strain rate hardening, the flow stress in the material increases and sawtooth chips are formed. The flow stress can be expressed as the formula of strain, strain rate, and temperature in the shear zone.

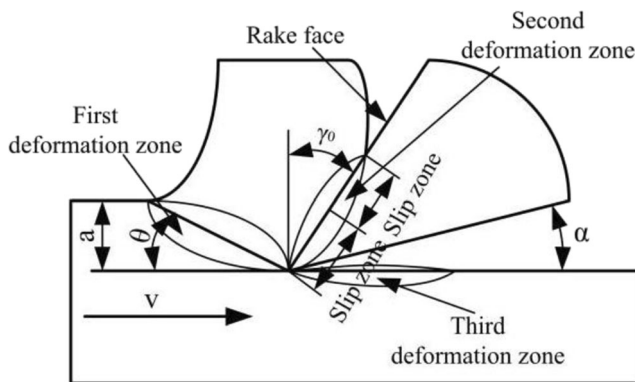


Fig. 1 Chip formation process

$$\tau = \tau(\gamma, \dot{\gamma}, T) \tag{1}$$

where  $\tau$  is flow stress,  $\gamma$  is strain,  $\dot{\gamma}$  is strain rate, and  $T$  is temperature.

Therefore, the adiabatic critical criterion for sawtooth chip generation is

$$0 \leq -\left(\frac{\partial \tau}{\partial \gamma}\right) / \left(\frac{\partial \tau}{\partial T} \times \frac{dT}{d\gamma}\right) \leq 1 \tag{2}$$

where  $\frac{\partial \tau}{\partial \gamma}$  refers to the strain hardening characteristics of materials;  $\frac{\partial \tau}{\partial T}$  refers to the thermal softening characteristics of materials; and  $\frac{dT}{d\gamma}$  refers to the rate of change of temperature with strain.

The critical condition for sawtooth chip generation is

$$\frac{d\tau}{dv} = \left(\frac{\partial \tau}{\partial \gamma} \cdot \frac{d\gamma}{dv}\right) + \left(\frac{\partial \tau}{\partial \dot{\gamma}} \cdot \frac{d\dot{\gamma}}{dv}\right) + \left(\frac{\partial \tau}{\partial T} \cdot \frac{dT}{dv}\right) = 0 \tag{3}$$

So the formula that affects the critical condition of sawtooth chip is

$$g(v) = \left(\frac{d\tau}{dv} + \frac{m}{n} \cdot \frac{d\dot{\gamma}}{dv}\right) - \left(\frac{c}{n} \cdot \frac{dT}{dv}\right) = 0 \tag{4}$$

where  $m$  is strain hardening rate;  $n$  is strain hardening coefficient; and  $C$  is thermal softening coefficient.

The relationship between the critical speed of sawtooth chip formation and strain, strain rate, and temperature is

$$g(v) = g_\gamma(v) + g_{\dot{\gamma}}(v) + g_T(v) \tag{5}$$

If the cutting speed reached the critical value, the effect of thermal softening was greater than that of strain rate hardening, causing serrated chip to form. When the cutting speed increased, the effect of thermal softening continued to increase, which made serration frequency of sawtooth chips increase. As a matter of fact, the critical speed leading to such serration was directly related to the strain, strain rate, and temperature in the shear zone. Therefore, serrated chip could be observed if changing strain, strain rate, or temperature at constant cutting speed.

### 2.2 Influence of ultrasonic-assisted milling on chip forming

In ultrasonic milling, when the cutting depth was greater than the axial ultrasonic amplitude, the cutting edge of the end face of the tool would not separate from the workpiece. The side edge was a spiral structure, and its side milling cutting model was simplified as shown in Fig. 2.  $O$  is the origin of the model,  $EF$  is the boundary of chip separation and the edge,  $\varphi$  is the helical angle

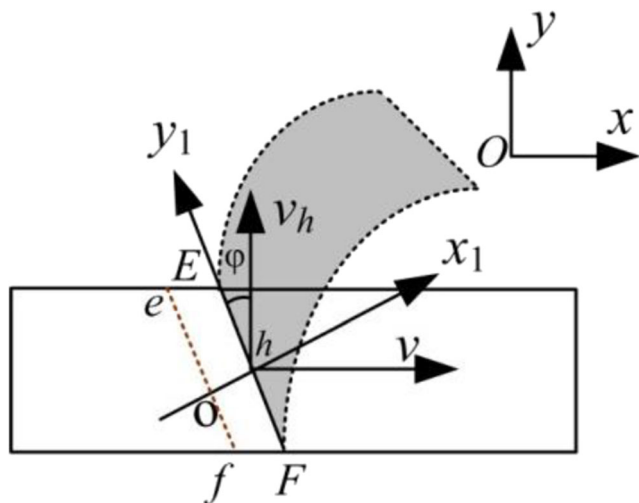


Fig. 2 Oblique cutting model

of the side edge of the tool,  $v_h$  is the axial vibration speed of the tool, and  $v$  is the cutting speed.

During ultrasonic vibration-assisted milling, the axial displacement of  $h$  at any point on the side cutting edge changing with time is

$$y_h = H + A \sin(2\pi ft + \phi_0) \tag{6}$$

where  $H$  is the initial height of  $h$  point;  $A$  is the ultrasonic amplitude;  $f$  is the ultrasonic vibration frequency;  $t$  is the time; and  $\phi_0$  is the initial phase. When the initial phase is zero, the relationship between the axial velocity  $v_h$  and time is

$$v_h = 2\pi f A \cos(2\pi ft) \tag{7}$$

As shown in Fig. 2, the cutting area of the cutting edge of the tool was simplified.  $EF$  is the boundary of chip separation and the edge, and the point  $h$  was set to the origin of coordinates, the line perpendicular to  $EF$  direction was the coordinate axis  $x_1$ , and the line along  $EF$  direction was the coordinate axis  $y_1$ . Specifying  $h$  point as the reference point, speed components in the  $x_1$  and  $y_1$  directions can be obtained by decomposing the cutting speed  $v$  and the axial speed  $v_h$  of the tool along the  $x_1$  and  $y_1$  directions respectively.

$$\begin{aligned} v_{x1} &= v \cos \phi + v_h \sin \phi \\ v_{y1} &= v_h \cos \phi - v \sin \phi \end{aligned} \tag{8}$$

Among them,  $v_p$ —sine changes, so the blade will vibrate periodically on both sides of  $EF$ . When  $v_{x1}$  is less than 0, the cutting edge moves to  $ef$ , which is separated from the chip  $EF$ , and finally, intermittent cutting is realized.

### 2.3 Mechanism of milling temperature rise

Figure 3 shows the simplified schematic diagram of milling temperature model. According to the model structure of milling cutter and cutting principle, the milling cutter can be divided into numerous units along the spiral edge when analyzing the cutting temperature produced in milling process. The cutting process of each unit can be simplified as oblique cutting. Figure 3a, b shows the temperature generated in the cutting area during milling. Results showed that temperature rise mainly occurred in three areas during milling, as shown in Fig. 3c including (1) cutting area of rake face where temperature rose resulting from friction behavior between chip and rake face; (2) cutting area of flank face where temperature increased due to friction between flank face and the workpiece; and (3) plastic deformation area of the shear surface where temperature increase occurred because of shear slip of the metal plastic deformation [7].

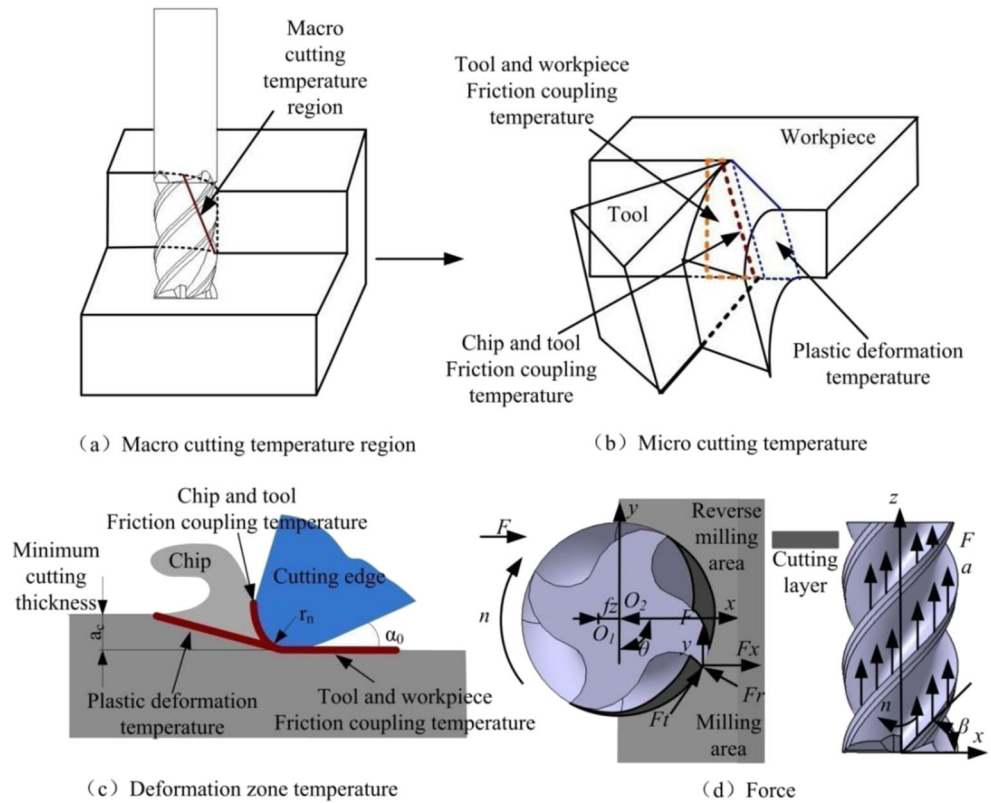
In the milling process, temperature was found to change with cutting thickness because the instantaneous cutting thickness of the tool spiral edge varied. As the milling cutter rotated during machining, the corresponding cutting thickness being machined by spiral edge was different. Meanwhile, the temperature streamline in the temperature rise area was non-uniform, and the cutting temperature along the helix changed continuously. Therefore, the temperature conduction of the spiral edge in the process of machining can be simplified as a length change [25].

## 3 Experimental analysis of tool wear mechanism in ultrasonic-assisted milling

### 3.1 Ultrasonic-assisted milling experimental platform

The ultrasonic-assisted milling device is mainly composed of transducer, horn, magnetic coil, and ultrasonic transmitter. A force platform and a temperature measuring instrument are installed on the work platform of the machine tool. Besides, an X-ray residual stress measuring instrument is available to measure the residual stress of the processed sample, and a scanning electron microscope is employed to present the morphological structures of chip and surface of the processed sample. A surface roughness meter is used to measure surface roughness of the treated sample. The experimental platform is shown in Fig. 4. In this paper, a TiSiN-coated end milling cutter with diameter of 6 mm, 4 edge, and helix angle of 45° was selected for the experiment, and parameters commonly used in rough machining and semi-finishing were as follows: ultrasonic-assisted amplitude  $A = 5 \mu\text{m}$ , frequency (25 kHz), the spindle speed  $n$

Fig. 3 Milling temperature model



= 4000 r/min, the feed speed  $f = 800$  mm/min, and the cutting depth  $a_p = 50 \mu\text{m}$ , as shown in Table 1. Table 2 shows Ti6Al4V performance parameters.

**3.2 Experimental detection and analysis of tool wear mechanism in ultrasonic-assisted milling**

The wear of milling cutter has three different stages during machining, namely, initial wear stage, normal wear stage, and severe wear stage. The initial wear stage is mainly determined by the manufacturing quality of the cutting edge. After rapid wear occurred, the cutting edge of the tool was sharpened leading to the normal wear stage. At the stage, the surface maintained a good quality, resulting in an optimal cutting surface. But as machining continued, tool wear began to deteriorate due to cutting vibration, temperature rise, and material hardening. In addition, melting or sticking phenomenon was observed as the temperature of the cutting area increased suddenly, and even cutting edge collapse occurred when reaching a limit value. As a result, the cutting requirements failed to be met. Figure 5 shows the morphological image of tool wear during ultrasonic-assisted milling.

The energy spectrum analysis was carried out on the damaged parts of the front and back face of the ultrasonic-assisted milling tool by using the scanning electron microscope to investigate the cause of tool wear, and the tool wear mechanism was explored by detecting changes in the element composition in a specific area. Figure 6 shows the wear morphology and EDS energy spectrum analysis of the front face of tool during ultrasonic-assisted milling of Ti6Al4V. The comparative analysis of elements at A and B of the front cutter face

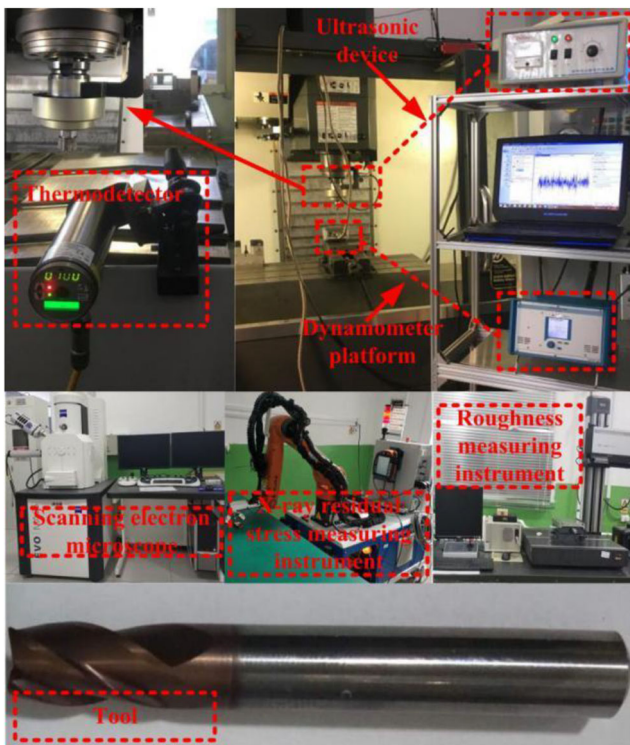


Fig. 4 Experimental platform

**Table 1** Tool wear test plan

Tool type	Diameter: 6 mm, 4 edge, a front angle of 30°, a back angle of 14°, and a helix angle of 45; surface coating: TiSiN carbide milling cutter	Equipment	Performance parameter
Spindle speed (r/min)	4000	Machining center	Spindle: 12,000 rpm; stroke: 762 * 406 * 508 mm
Feed rate (mm/min)	800		
Cutting depth (μm)	50	Dynamometer	Force measuring range: $F_x, F_y, F_z - 250\sim 250$ N
Steps (%)	Diameter × 50%	Scanning electron microscope	Maximum magnification: 50,000 times
Milling method	Down milling		
Tool wear time (min)	10, 20, 30, 40, 50, 60, 70	X-ray residual stress measuring instrument	Measuring angle: 0°, ± 15°, ± 45°, ± 60°
Frequency (kHz)	25		
Ultrasonic amplitude (μm)	A = 5	Surface roughness meter	Measuring range: ± 250 μm

indicated that a certain number of tungsten, cobalt, nitrogen, and oxygen elements were detected at A area of the cutter tip, and the content of tungsten and cobalt elements in the cutter base increased. It can be explained that the matrix elements were exposed to air because the tool coating were worn off, and oxidation wear occurred in the area of the front tool surface during the milling process of Ti6Al4V as oxygen element was found at the A area of the cutter tip, as shown in Fig. 6b. However, the energy spectrum analysis illustrated that the element composition of B area, far away from the tool tip, did not change, indicating that no tool wear happened, as shown in Fig. 6c. On the other hand, adhesion wear occurred in the narrow area between the front face and the cutting edge because the front face of the tool was bonded.

Figure 7 shows the wear morphology and EDS energy spectrum analysis of the back face of tool in ultrasonic-assisted milling of Ti6Al4V. The results of comparative analysis of elements at A and B of back cutter face indicated that a certain content of titanium element was observed at A area of the cutter tip and the content of titanium element increased sharply while the content of nitrogen element in cutter base decreased, as shown in Fig. 7b. It can be proved that diffusion wear occurred in the area of the back face during milling. However, the element composition at B area, far away from the tool tip, did not change based on the energy spectrum analysis, indicating that no wear occurred in this area, as shown in Fig. 7c.

**Table 2** Property parameters of Ti6Al4V

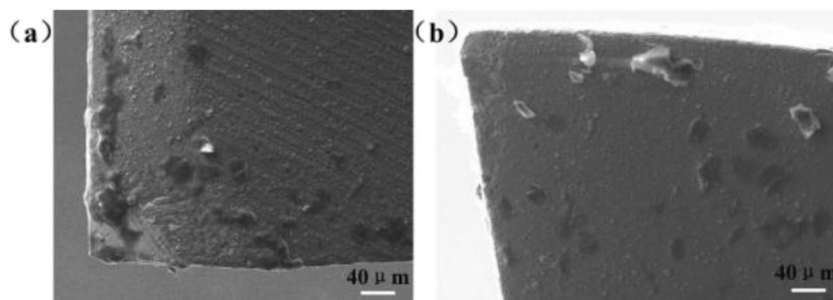
Density (kg/m <sup>3</sup> )	4440
Modulus of elasticity (GPa)	640
Hardness (HV)	340.6
Poisson's ratio	0.33
Yield strength (GPa)	835
Thermal conductivity (W m/K)	6.8

In Figs. 6 and 7, a certain number of titanium and oxygen elements were found on the surface of the notch in the wear area of the ultrasonic-assisted milling tool. The wear area of the cutting edge of the front face was narrow and the front face of the tool was bonded. Meanwhile, results indicated that the content of W and CO increased, and the content of Ti at tool face increased after ultrasonic-assisted milling. It can be proved that during ultrasonic-assisted milling of Ti6Al4V, oxidation wear, adhesive wear, and diffusion wear occurred. In conclusion, the wear mechanism of cemented carbide coated tool in milling Ti6Al4V mainly included oxidation wear, adhesion wear, and diffusion wear.

### 3.3 Comparative analysis of tool wear in ultrasonic-assisted milling and conventional milling

Cutting parameters,  $n = 4000$  r/min,  $F = 800$  mm/min,  $a_p = 50$  μm, are commonly used during roughing and semi-finishing of Ti6Al4V. Figure 8 shows the change rule of the maximum wear of the back face of the cutter with the tool wear time when machining Ti6Al4V with two milling approaches under these parameters. It can be seen in the figure that tool wear during ultrasonic-assisted milling was far less than that of conventional milling, resulting in longer service life. Specifically, in conventional milling, the initial wear stage, the normal wear stage, and the severe wear stage occurred in 0–10 min, 10–40 min, and 40–50 min, respectively, and tool tipping was observed after milling for 50 min. However, using ultrasonic-assisted milling method, the three stages were found in 0–5 min, 5–50 min, and 50–70 min, respectively, and edge collapse occurred after milling for 70 min. Compared to conventional milling, it can be explained that in ultrasonic-assisted machining, the cutting tool is conducive to material shear slip, and ultrasonic is capable of effectively inhibiting the phenomenon of chip sticking in the process of chip separation of titanium alloy materials, which not only allows more effective chip discharge

**Fig. 5** Wear morphology of cutting tools in ultrasonic-assisted milling. **a** The front cutter face is worn. **b** The rear cutter face is worn



as compared to conventional milling method but requires less cutting force resulting in lower temperature.

## 4 Analysis of the influence of tool wear on cutting process

### 4.1 Influence of tool wear time of different milling methods on chip

Tool wear has a direct impact on chip shape. Chip formation is actually caused by tool extrusion. When the material is squeezed by the tool, the crystal lattice inside the material will be sheared and slip to form chips. When the material is affected by the external force of the tool, the internal grain stress and strain begin to increase, and when the internal stress reaches the yield point of the material, slip begins to occur. The micro-morphology of chips and chips formed by two different cutting conditions at different wear time is shown in Fig. 9. It can be found that the

cutting curl angle of ultrasonic-assisted milling is much smaller than that of conventional milling at the same wear time by comparing the chips produced by ultrasonic-assisted milling and conventional milling tools. This is because the cutting tool can restrain the chip sticking phenomenon under the assistance of ultrasonic vibration, and the generated cutting force and cutting temperature will be relatively low, which is conducive to chip forming. Therefore, compared with conventional milling conditions, it is more conducive to shear slip and chip outflow, and the chip curl angle is smaller.

### 4.2 Influence of tool wear on cutting force in ultrasonic-assisted milling

The degree of tool wear has a direct effect on the cutting force produced in the cutting process. Figure 10 shows the cutting diagram when the tool wear time of ultrasonic-assisted machining is 5–70 min. As the tool wear continued, the cutting force obtained in each stage gradually became larger. As a

**Fig. 6** a–c Wear morphology and EDS energy spectrum analysis of the front face of tool in ultrasonic-assisted milling of Ti6Al4V

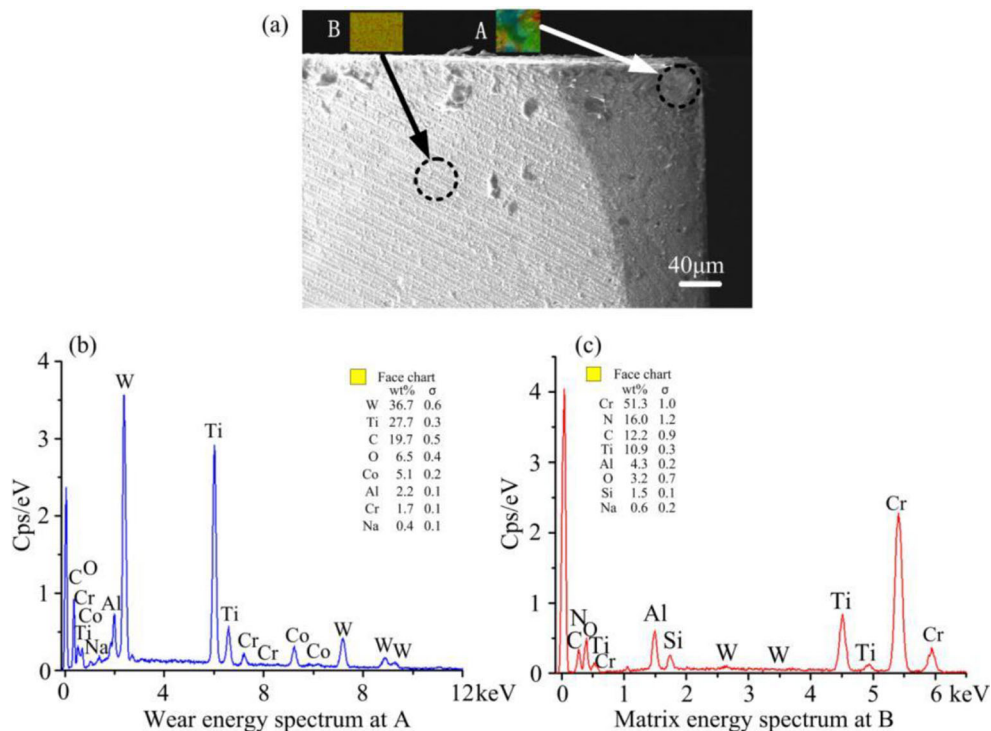
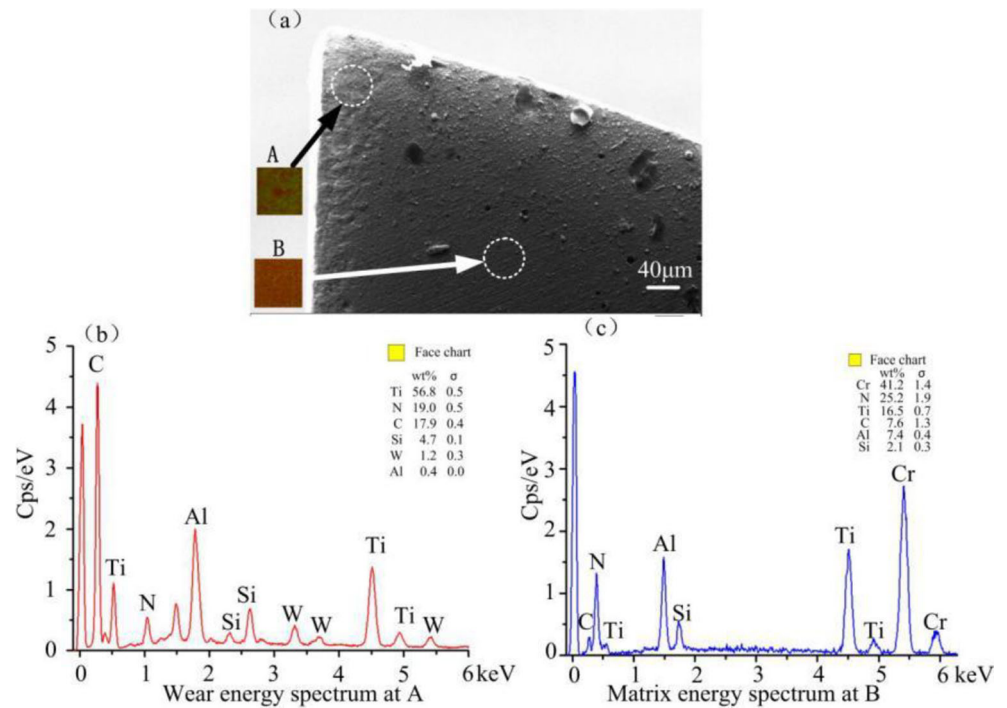


**Fig. 7 a–c** Wear morphology and EDS energy spectrum analysis of cutting surface of tool in ultrasonic-assisted milling of Ti6Al4V



matter of fact, the tool wear is directly related to the performance of chip separation during cutting. The severer the wear is, the greater the friction between the front and back face of the tool and the cutting layer causing higher temperature. However, when the tool wear time reached 50–70 min, the tool wear began to deteriorate. At this stage, the tool edge wear deteriorated sharply, and adhesion was observed on the front and rear tool faces of the tool or even edge breakage occurred. As a result, the friction between the tool and the cutting layer increased sharply and hence the temperature became higher causing the chip separation to fail to reach a stable state and finally cutting force increased accordingly. Compared to conventional milling, in ultrasonic-assisted machining, the cutting tool is conducive to material shear slip, and ultrasonic is

capable of effectively inhibiting the phenomenon of chip sticking in the process of chip separation of titanium alloy materials, which not only allows more effective chip discharge as compared to conventional milling method but requires less cutting force resulting.

### 4.3 Influence of tool wear on residual stress of cutting surface in ultrasonic-assisted milling

It can be seen in Fig. 11 that when the tool wear time was 5–70 min, the residual stress of machined surface layer showed an increasing trend. This is because the degree of tool wear is directly related to the stability of chip separation during cutting. The severer the wear is, the greater the

**Fig. 8** Comparison between the maximum wear on the back face of the cutter and the milling time at each time when machining Ti6Al4V

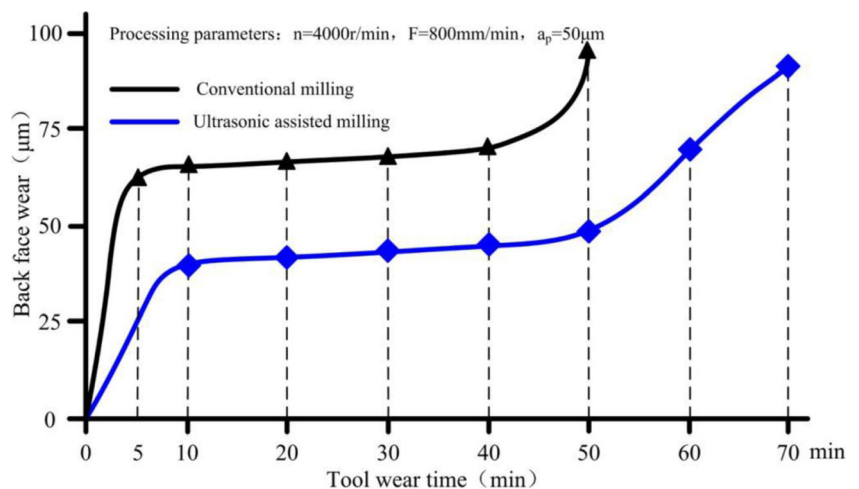
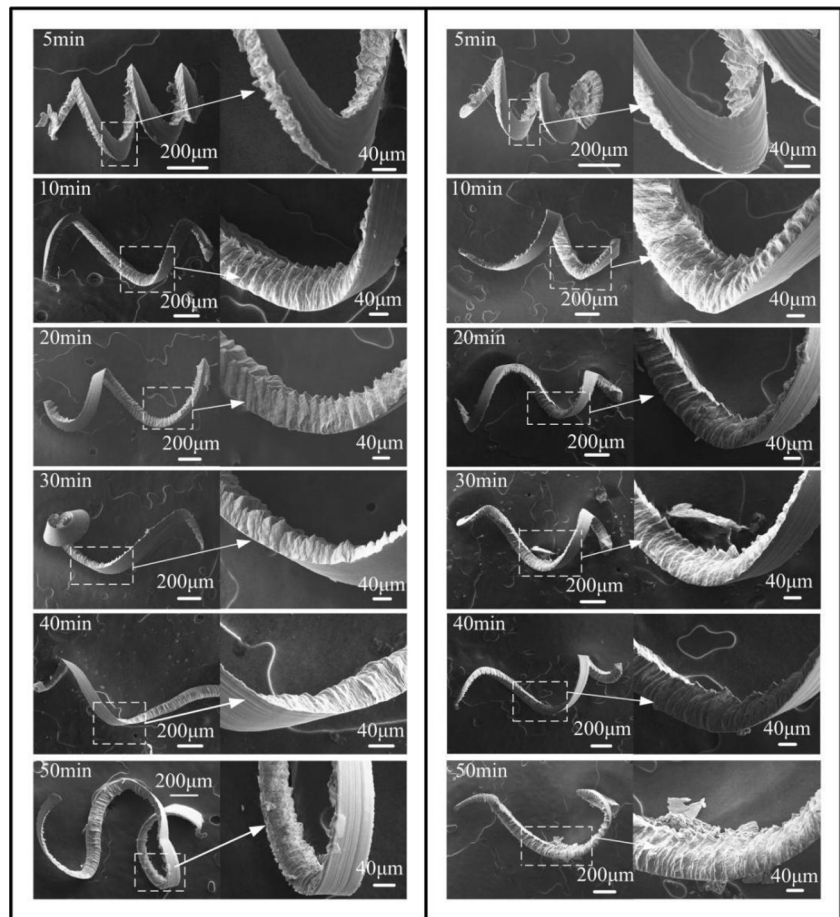


**Fig. 9** Influence of tool wear time of different milling methods on chip forming under  $n = 4000$  r/min,  $F = 800$  mm/min, and  $a_p = 50$   $\mu\text{m}$ . **a** Conventional milling. **b** Ultrasonic-assisted milling



(a) Conventional milling;

(b) Ultrasonic assisted milling.

friction between the cutting edge and the cutting layer. Consequently, the cutting force becomes greater and the temperature increases at the interface between cutting edge and the cutting layer, leading to a greater pressure stress on the machined surface. However, when the tool wear time reaches 50–70 min, the tool is in the stage of severe wear. Under these circumstance, the cutting edge wear increases sharply, which leads to sharp increase of friction between the tool and the cutting layer, and hence the temperature rises and the chip separation fails to reach a stable state, causing higher residual stress on the machined surface. It can be seen from the figure that the surface residual stress of conventional milling is the same when the cutting time is the same. Because that in ultrasonic-assisted machining, the cutting tool is conducive to material shear slip, and ultrasonic is capable of effectively inhibiting the phenomenon of chip sticking in the process of chip separation of titanium alloy materials, which not only allows more effective chip discharge as compared to conventional milling method but requires less cutting force resulting in lower temperature. Therefore, ultrasonic-assisted milling has less

influence on the internal stress distribution than conventional milling.

#### 4.4 Influence of tool wear on cutting surface roughness in ultrasonic-assisted milling

The degree of tool wear is directly related to the surface roughness of machined parts. In Fig. 12, under ultrasonic-assisted milling, it can be seen that as tool wear time increases, the machined surface roughness at each stage decreases first and then increases. This is because when the tool wear time is 5 min, the tool is in the initial wear stage which is not the optimal cutting stage due to the height difference between the blades and hence the optimum surface roughness is not obtained. However, when the tool wear time is 50–70 min, the tool wear becomes deteriorated severely, causing the surface roughness to increase dramatically. This is because when machining for 50 min, the tool is at the critical stage of normal wear and severe wear. Under the circumstances, the tool edge suffers from severe wear, and hence the friction between the blade surface and the cutting layer becomes larger, leading to



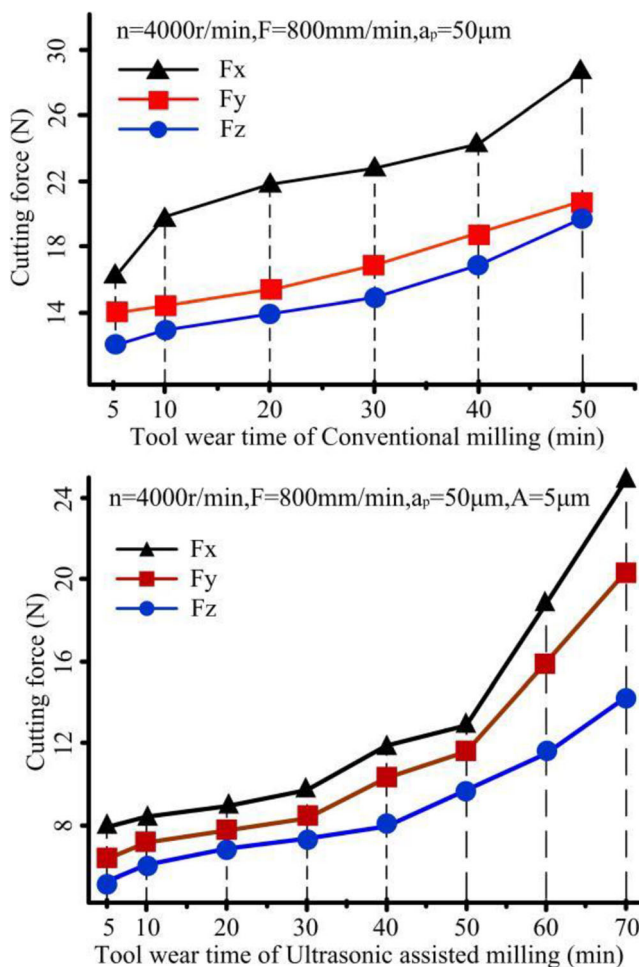


Fig. 10 Influence of different tool wear times on cutting force

an ineffective chip separation. Therefore, when the tool wear time is 50 min, the surface roughness of the machined surface begins to increase dramatically. As can be seen from Fig. 12, under the same processing time, compared with the surface roughness value obtained by conventional milling, it is found

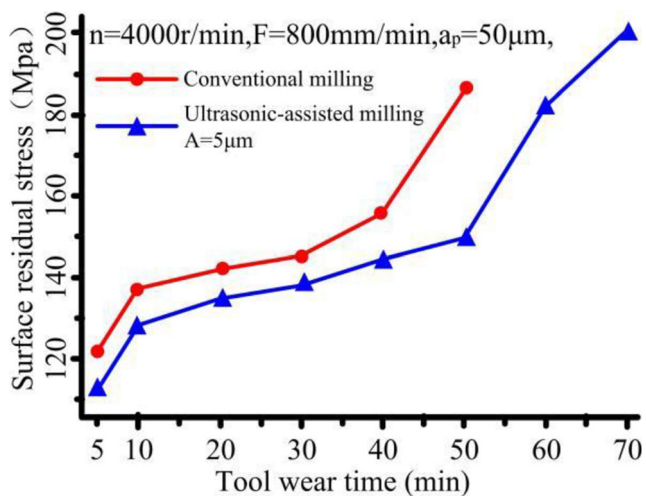


Fig. 11 Influence of tool wear time on residual stress of cutting surface

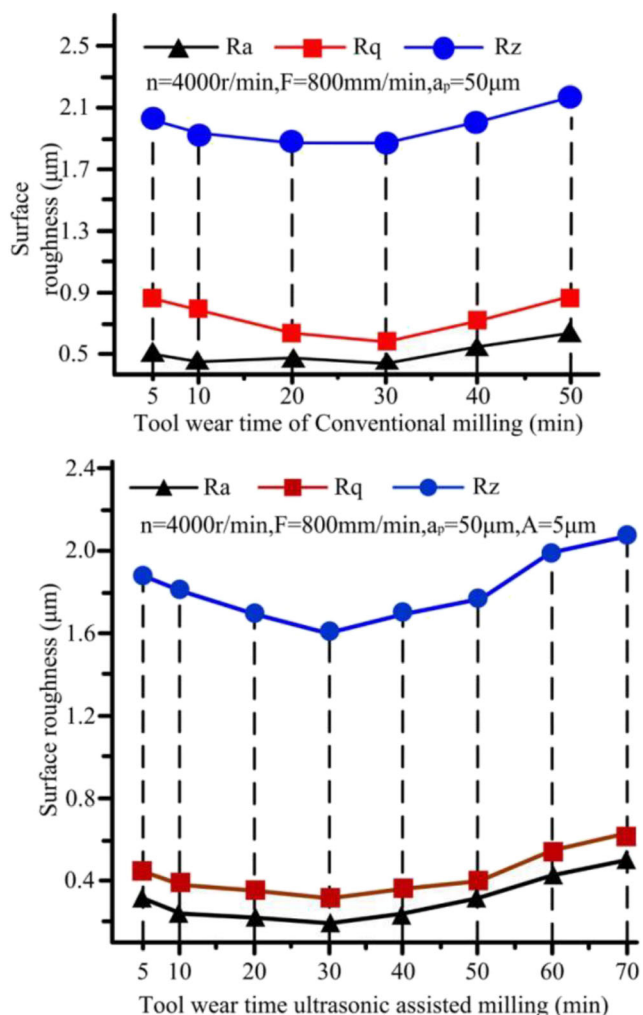


Fig. 12 Influence of tool wear time on cutting surface roughness

that the surface roughness obtained by ultrasonic-assisted milling is significantly smaller. This is because the milling tool can inhibit chip bonding phenomenon under the assistance of ultrasonic vibration, which is conducive to chip forming, and the friction between the tool and chip on the workpiece is smaller, so the surface roughness value obtained by conventional milling is significantly smaller.

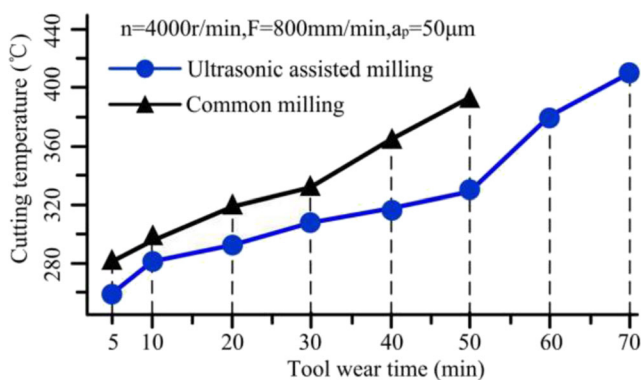
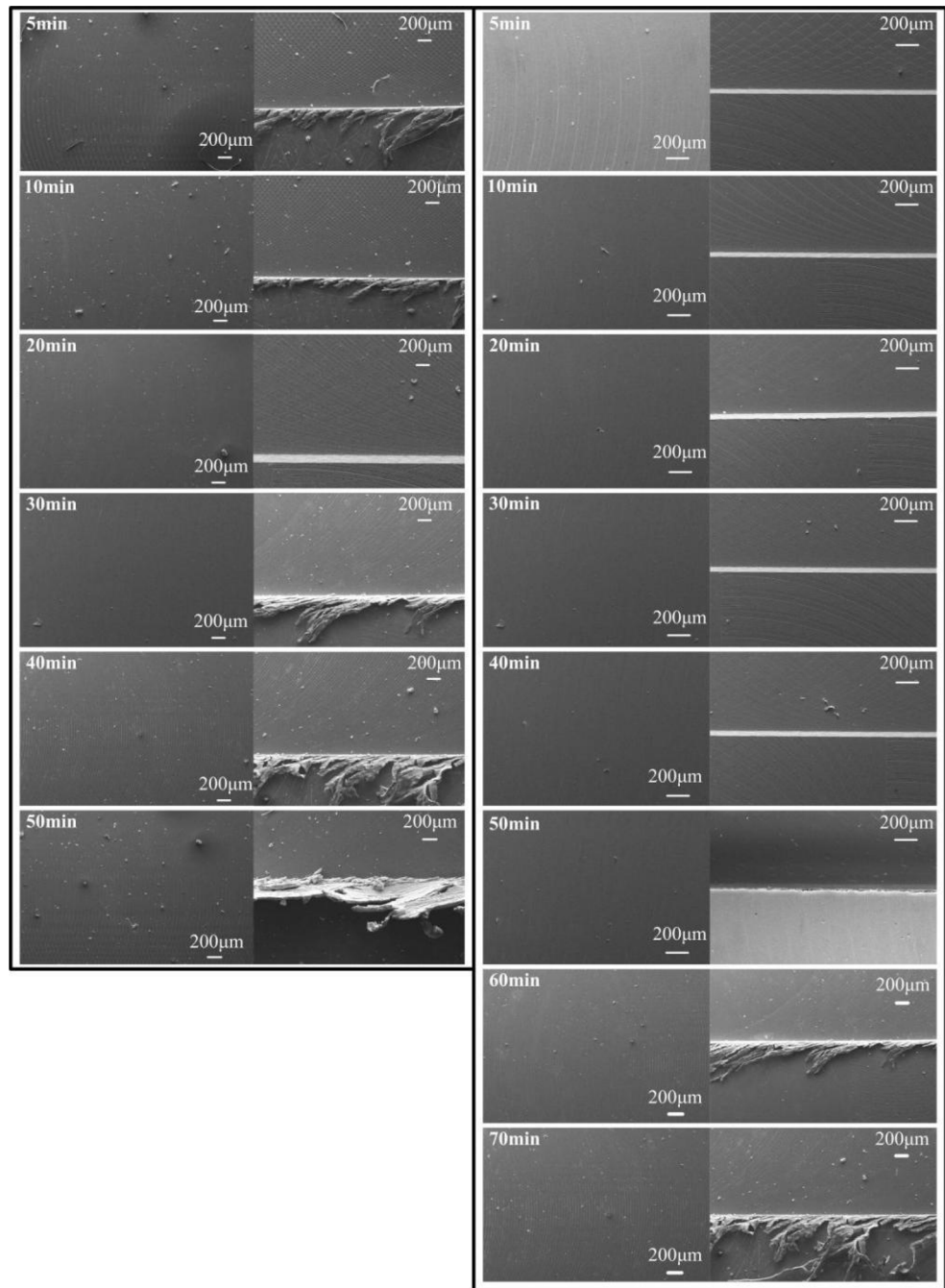


Fig. 13 Influence of different wearing tools on cutting temperature

**Fig. 14** Surface morphology of different worn tools under  $n = 4000$  r/min,  $F = 800$  mm/min, and  $a_p = 50$   $\mu\text{m}$ . **a** Conventional milling. **b** Ultrasonic-assisted milling



(a) Conventional milling;

(b) Ultrasonic assisted milling.

#### 4.5 Influence of tool wear on cutting temperature in ultrasonic-assisted milling

In the process of machining, the cutting temperature at the tool tip directly affects the service life of the tool. In Fig. 13, it can be observed that the cutting temperature gradually increases when the tool wear time is 5–70 min. This is because the degree of tool wear is directly related to the performance of chip separation during cutting. The severer the wear is, the

greater the friction between the blade and the cutting layer in a certain time, causing higher temperature at the tool tip. However, when the tool wear time reaches 50–70 min, the tool is in the stage of severe wear, in which the blade wear increases sharply, which leads to sharp increase of friction between the tool and the cutting layer. As a result, increased friction has a negative impact on the effectiveness of chip separation, impeding thermal dissipation in a timely manner. Therefore, the cutting temperature rises sharply.

## 4.6 Influence of tool wear on cutting surface quality

Tool wear is directly related to the surface quality of the machined part. As shown in Fig. 14, the comparative results of the two machining methods under the same tool wear time showed that in conventional milling, cutting mark on machined surface was obvious and the edge burr was large, and the chip adhesion phenomenon was observed on the machined surface. This is because the cutting force generated in conventional milling was great resulting in a higher temperature. By contrast, the cutting force under the assistance of ultrasonic vibration was relatively low, and ultrasonic vibration coupling was more conducive to shear slip and chip discharge, obtaining smaller edge burr. On the other hand, the best surface quality was obtained at the normal wear stage in both conventional and ultrasonic-assisted milling. It can be explained that height difference between the cutting edges at the initial wear stage of the tool caused unsatisfied cutting coupling state, so the cutting marks on the machined surface and edge burr were relatively obvious. Furthermore, as the tool became deteriorated severely, the quality of the machined surface started getting worse. This is because the tool edge suffered from a severe wear at this stage, and hence the friction between the blade surface and the cutting layer increased resulting in temperature rise; as a result, ineffective chip separation occurred and the surface quality was greatly affected exhibiting large burr at the edge of separation. However, when it came to the normal wear stage, the machined surface quality was gradually smooth.

## 5 Conclusions

Based on the study and investigations, the following conclusions can be drawn:

1. Considering the results of energy spectrum analysis of the damaged parts of the cutting tool front and back and changes in element composition in specific areas, oxidation wear, adhesion wear, and diffusion wear were observed for the tool in ultrasonic-assisted milling of Ti6Al4V.
2. In the ultrasonic-assisted milling process, improved tool service life was obtained as compared to the conventional milling method.
3. At the same wear time, the curl angle of chip generated from ultrasonic-assisted milling was smaller and the edge burr was not obvious as compared to that of conventional milling.
4. Compared with the conventional method, lower cutting force and temperature as well as improved surface roughness were obtained in ultrasonic-assisted milling at the same wear time.

**Acknowledgments** The authors sincerely thank Professor Hua-dong Yu of Changchun University of Science and Technology for his critical discussion and reading during manuscript preparation.

**Funding information** This work was supported by “Supported by national basic scientific research program” (JCKY2017208B006).

## References

1. Guang CHEN, Zhihong KE, Chengzu REN, Jun LI (2016) Constitutive modeling for Ti-6Al-4V alloy machining based on the SHPB tests and simulation [J]. *Chin J Mech Eng* 29:962–970
2. Ulutan D, Ozel T (2011) Machining induced surface integrity in titanium and nickel alloys: a review. *Int J Mach Tool Manu* 51:250–280
3. Mhamdi MB, Boujelbene M, Bayraktar E (2012) Surface integrity of titanium alloy Ti-6Al-4V in ball end milling. *International Conference on Solid State Devices and Materials Science Physics Procedia* 2012(25):355–362
4. Su HH, Liu P, Fu YC (2012) Tool life and surface integrity in high-speed milling of titanium alloy TA15 with PCD/PCBN tools [J]. *Chin J Aeronaut* 25:784–790
5. Ezugwu EO, Bonneya J, Silvab RBD (2007) Surface integrity of finished turned Ti-6Al-4V alloy with PCD tools using conventional and high pressure coolant supplies. *J Mach Tools Manu* 47:884–891
6. Zhao B, Li PT, Zhang CY et al (2019) Effect of ultrasonic vibration direction on milling characteristics of TC4 titanium alloy [J]. *Acta Aero-nautica et Astronautica Sinica*:40
7. Liu J L, Zhang B, Bai Q, et al. Temperature prediction of tool/workpiece contact zone in titanium milling [J]. *Acta Aero-nautica et Astronautica Sinica*, 2018,39(12): (in Chinese).
8. Guo J, Jianguo Z, Pan Y, Renke K et al (2019) A critical review on the chemical wear and wear suppression of diamond tools in diamond cutting of ferrous metals. *Int J Extrem Manuf*:01
9. Dong G, Wang X, Gao S (2018) Molecular dynamics simulation and experiment research of cutting-tool wear mechanism for cutting aluminum alloy. *Int J Adv Manuf Technol* 96(1-4):1123–1137
10. Rehman GU, Jaffery SHI, Khan M, Ali L, Khan A, Ikramullah Butt S (2018) Analysis of burr formation in low speed micro-milling of titanium alloy (Ti-6Al-4V). *Mech Sci* 9(2):231–243
11. Ambati R, Huang Y (2011) FEM mesh-dependence in cutting process simulations. *Int J Adv Manuf Technol* 53:313–323
12. Yong-hong FU, Kai-long XIAO, Xi-jun HUA et al (2013) Cutting trial and performance analysis of surface micro-grooves turning tools [J]. *China Surf Eng* 26(6):106–111.45 (4) : 529-535
13. Xie J, Luo MJ, Wu KK et al (2013) Experimental study on cutting temperature and cutting force in dry turning of titanium alloy using anon-coated micro-grooved tool [J]. *Int J MachTools Manu* 73:25–26
14. Wang Q, Liu Z (2016) Evolutions of grain size and micro-hardness during chip formation and machined surface generation for Ti-6Al-4V in high-speed machining. *Int J Adv Manuf Technol* 82:1725–1736
15. Ding R, Guo ZX (2004) Microstructural evolution of a Ti-6Al-4V alloy during  $\beta$ -phase processing: experimental and simulative investigations. *Mater Sci Eng A* 365:172–179
16. Rotella G, Umbrello D (2014) Finite element modeling of micro-structural changes in dry and cryogenic cutting of Ti6Al4V alloy. *CIRP Ann Manuf Technol* 63:1–4
17. Qiang LIU, Huan LIU, Songmei YUAN (2016) High accurate interpolation of NURBS tool path for CNC machine tools [J]. *Chin J Mech Eng* 29:911–920

18. Chen T, Song L, Li S, Liu X (2019) Experimental study on wear characteristics of PCBN tool with variable chamfered edge [J]. *Chin J Mech Eng*:32–37
19. Weinert K, Biermann D, Bergmann S (2007) Machining of high strength light weight alloys for engine applications [J]. *Annals of the CIRP* 56(1):105–108
20. Ming C, Ya-dong G, Ning Y et al (2017) Experimental study on surface quality of single crystal DD98 in micro-milling processes [J]. *China Mech Eng* 28(11):1261–1265
21. Chen G, Ren CZ, Yang XY, Jin XM, Guo T (2011) Finite element simulation of high-speed machining of titanium alloy (Ti-6Al-4V) based on ductile failure model. *Int J Adv Manuf Technol* 56:1027–1038
22. Shi Q, He N, Li L (2012) Analysis on surface integrity during high speed milling for new damage tolerant titanium alloy. *Transaction of Nanjing University of Aeronautics and Astronautics* 29(3):222–226
23. Ming L, Jing W, Baohai W, Dinghua Z (2017) Effects of cutting parameters on tool insert wear in end milling of titanium alloy Ti6Al4V [J]. *Chin J Mech Eng* 30:53–59
24. Khan MA, Jaffery SHI (2019) Statistical analysis of energy consumption, tool wear and surface roughness in machining of titanium alloy (Ti-6Al-4V) under dry, wet and cryogenic conditions[J]. *Mech Sci* 10:561–573
25. Li GC, Sun J, Li JF, Song LY, Li WD (2014) Accurate 3D modeling and software implementation of end mill [J]. *J Comput Aided Des Comput Graph* 3(26):(in Chinese)

**Publisher's note** Springer Nature remains neutral with regard to jurisdictional claims in published maps and institutional affiliations.